

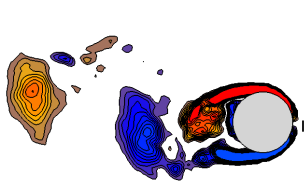
High-order Spectral Difference Method for Simulating Unsteady Flow past a plunging airfoil



Antony Jameson, Chunlei Liang

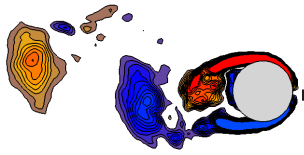
**Aeronautics and Astronautics
Stanford University**

Vortex dominated flow workshop
National Institute of Aerospace
Virginia, June, 2009



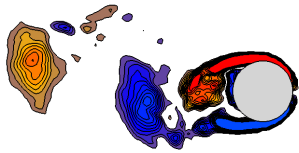
OVERVIEW

- **Introduction**
- **Spectral Difference method**
- **Validation**
- **Vortex Shedding**
- **Subsonic Flow past a plunging airfoil**



Higher order Methods (DG,SV,SD)

- Low numerical dissipation
- Less numerical dispersion
- Unstructured grids
- CPU efficient/easy to parallelize
- Not memory intensive
- Easy to program, universal construction by placing unknown points in a geometrical similar manner
- SD attains a simpler form and higher efficiency than DG and SV.
- Flexible (grid-independence, hp adaptation, moving boundary, deformable grid)



History of Spectral Difference Method

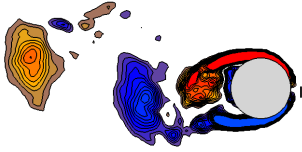
Two early papers on the SD method

- D. A. Kopriva and J. H. Kolas, A conservative staggered-grid chebyshev multidomain method for compressible flows. J. Comput. Phys. 125 (1996), p. 244. **STRUCTURED STAGGERED GRID**
- Yen Liu , Marcel Vinokur , Z. J. Wang, Spectral difference method for unstructured grids I: basic formulation, Journal of Computational Physics, v.216 p.780-801,2006. **UNSTRUCTURED MULTIVARIATE FORMULATION**

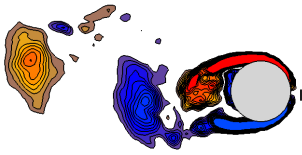
Our papers on the SD method

- Wang, Z.J., Liu, Y., May, G., Jameson, A.: "Spectral Difference Method for Unstructured Grids II: Extension to the Euler Equations" , J. Sci. Comput. 32 (1) pp. 54-71, July, 2007. **EXTENSION TO EULER EQUATIONS**
- C. Liang, S. Premasathan, A. Jameson, "High-order accurate simulation of flow past two side-by-side cylinders with Spectral Difference method", 2009, vol 87, pp. 812-817, Journal of Computers and Structures. **EXTENSION TO 2D Viscous flow on quadrilateral elements**
- C. Liang, A. Jameson and Z. J. Wang, "Spectral Difference method for two-dimensional compressible flow on unstructured grids with mixed elements", Journal of Computational Physics, vol 228, pp 2847-2858, 2009. **EXTENSION TO 2D Viscous flow on mixed elements**

Development of the spectral difference method in Stanford University



- 2D quadrilateral/triangular element
- 3D hexahedral elements
- 4th-order and higher on unstructured grids
- Implicit LU-SGS time stepping
- P-multigrid method
- Moving and deforming grids
- Artificial viscosity for shock capturing
- Parallelization (MeTis/MPI) of 3D code



High-order spectral difference method

□ The figure shows one way to locally construct a third-order spectral difference scheme for a grid cell.

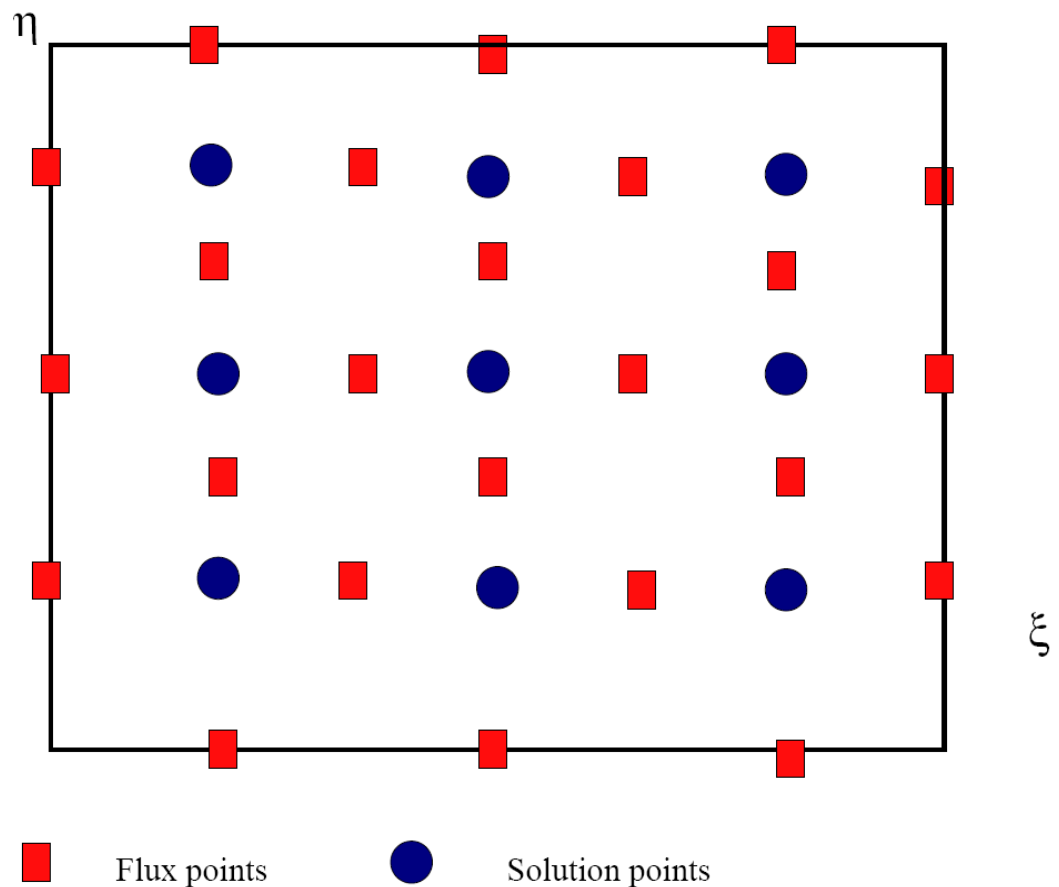
□ 9 solution points are used.

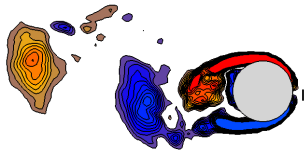
□ 24 flux points are employed.

□ The reconstructed field using polynomials is continuous within the cell but discontinuous across the cell boundaries

- Flux points store $f(q)$
- Solution points store q

$$\frac{dq}{dt} + df(q)/dx = 0$$





Choosing solution and flux points

- N solution points (one can choose arbitrarily)

(a)
$$X_s = \frac{1}{2} \left[1 - \cos \left(\frac{2s-1}{2N} \cdot \pi \right) \right], s = 1, 2, \dots, N.$$
 Gauss points

- N+1 flux points

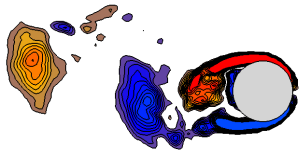
(b)
$$X_{s+1/2} = \frac{1}{2} \left[1 - \cos \left(\frac{s}{N} \cdot \pi \right) \right], s = 0, 1, \dots, N.$$
 Chebyshev-Gauss-Lobatto points

Or

(c) Roots of the equation: $P_n(\xi) = 0$ Legendre-Gauss quadrature points and two end points of 0 and 1.

$$P_{-1}(\xi) = 0$$

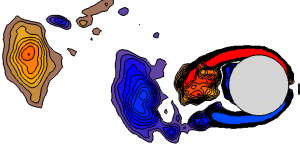
$$P_0(\xi) = 1 \quad P_n(\xi) = \frac{2n-1}{n} (2\xi-1) P_{n-1}(\xi) - \frac{n-1}{n} P_{n-2}(\xi)$$



Stability of the Spectral Difference method

- K Abeele, C Lacor and Z. J. Wang (2008), *On the stability and accuracy of the spectral difference method*, Journal of Scientific Computing, vol 37, pp. 162-188.
- Antony Jameson, (2009), *A proof of the stability of the spectral difference method for all orders of accuracy*, Aerospace Computing Lab report, ACL-2009-1, Stanford University, March 2009.
- Both confirm stability when the interior flux points are at the zeros of the **Legendre polynomial**

Solution and Flux reconstruction



Degree N-1 polynomial through solution points using Lagrange basis polynomial

$$h_i(X) = \prod_{s=1, s \neq i}^N \left(\frac{X - X_s}{X_i - X_s} \right)$$

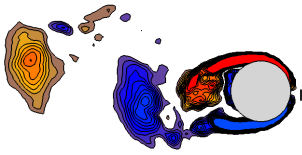
Degree N polynomial through flux points using Lagrange basis polynomial

$$l_{i+1/2}(X) = \prod_{s=0, s \neq i}^N \left(\frac{X - X_{s+1/2}}{X_{i+1/2} - X_{s+1/2}} \right)$$

Reconstructed solution as well as flux polynomials within an element are written as tensor products of three 1D polynomials

$$Q(\xi, \eta, \beta) = \sum_{k=1}^N \sum_{j=1}^N \sum_{i=1}^N \frac{\tilde{Q}_{i,j,k}}{|J_{i,j,k}|} h_i(\xi) \cdot h_j(\eta) \cdot h_k(\beta)$$

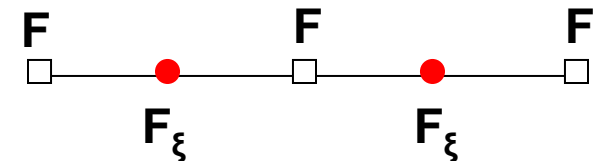
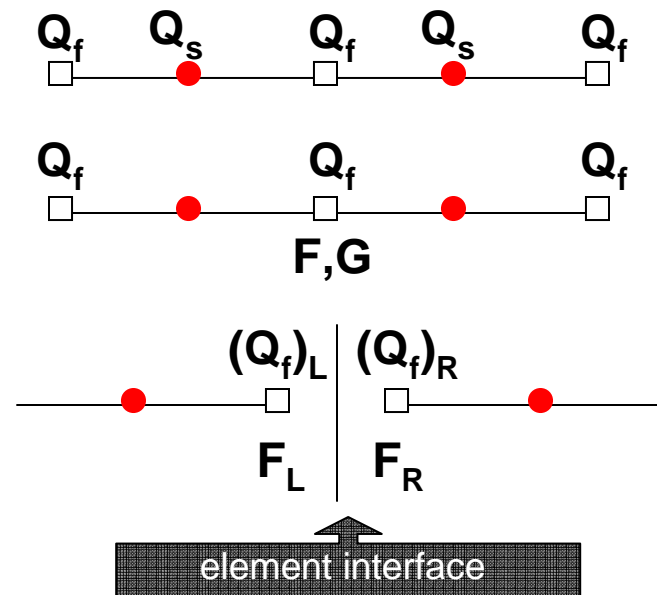
$$\tilde{F}(\xi, \eta, \beta) = \sum_{k=1}^N \sum_{j=1}^N \sum_{i=0}^N \tilde{F}_{i+1/2,j,k} l_{i+1/2}(\xi) \cdot h_j(\eta) \cdot h_k(\beta)$$

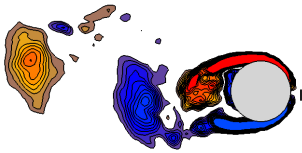


Calculation of inviscid flux derivatives

- Given the conservative variables at the solution points, the conservative variables are extrapolated to the flux points
- The inviscid fluxes at the interior flux points are computed
- The inviscid fluxes at the element interfaces are computed using an approximate Riemann solver
- The derivative of the fluxes are computed at the solution points according to

$$\left(\frac{\partial \tilde{F}}{\partial \xi} \right)_{i,j} = \sum_{r=0}^N \tilde{F}_{r+1/2,j} \cdot l'_{r+1/2}(\xi_i)$$

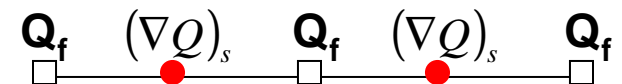
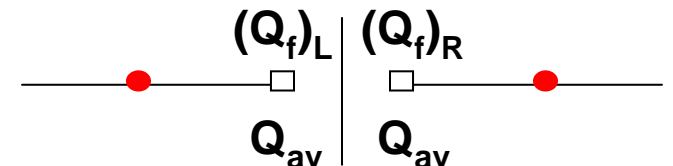
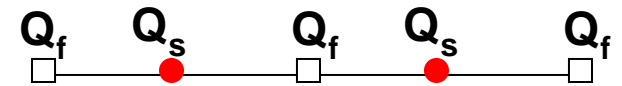


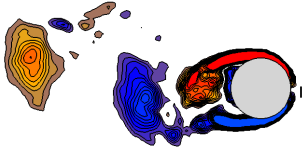


Calculation of viscous flux derivatives (1)

- ❑ The viscous fluxes depend on both the solution and the solution gradient at the flux points
- ❑ Reconstruct conservative variables at flux points using values at solution points
- ❑ At flux points on element interfaces, compute the average of left and right solution values
- ❑ Calculate the gradient of Q at the solution points from Q at flux points

$$F_v = F_v(Q_f, \nabla Q_f)$$





Calculation of viscous flux derivatives (2)

- Reconstruct ∇Q from solution points to flux points
- At flux points on element interfaces, compute the average of left and right ∇Q values
- Compute viscous fluxes at flux points
- Compute viscous flux derivatives at solution points
- We are ready to compute the NS equation, using a five-stage R-K scheme

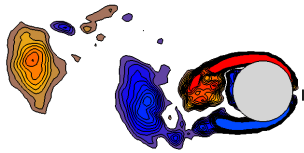
$$\frac{\partial Q}{\partial t} + \nabla F_e(Q) - \nabla F_v(Q, \nabla Q) = 0$$

$$(\nabla Q)_f \quad (\nabla Q)_s \quad (\nabla Q)_f \quad (\nabla Q)_s \quad (\nabla Q)_f$$

$$\frac{(\nabla Q)_L}{(\nabla Q)_{av}} \quad \bigg| \quad \frac{(\nabla Q)_R}{(\nabla Q)_{av}}$$

$$(\nabla Q)_f \quad F_v \quad (\nabla Q)_f \quad F_v \quad (\nabla Q)_f$$

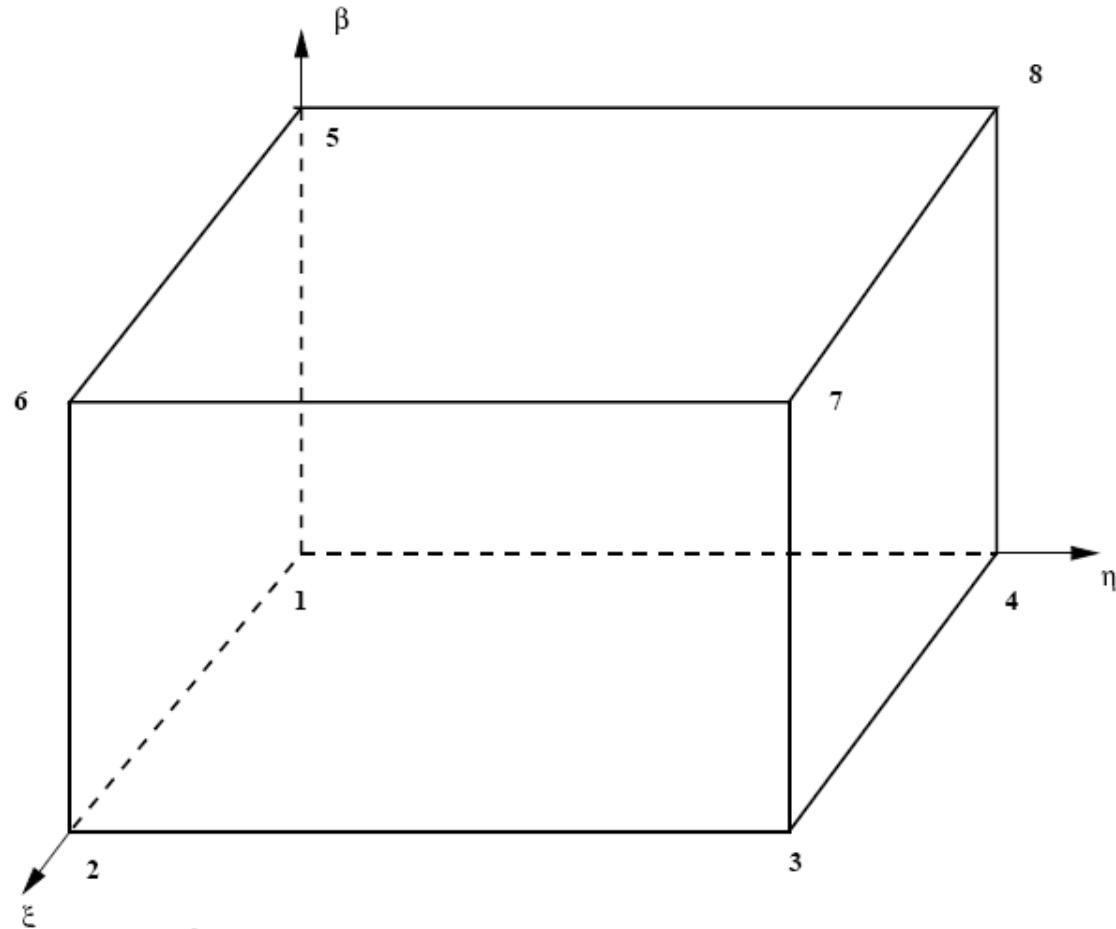
$$F_v \quad (F_v)_\xi \quad F_v \quad (F_v)_\xi \quad F_v$$



Hexahedral grid mapping

$$\begin{pmatrix} x \\ y \\ z \end{pmatrix} = \sum_{i=1}^K M_i(\xi, \eta, \beta) \begin{pmatrix} x_i \\ y_i \\ z_i \end{pmatrix}$$

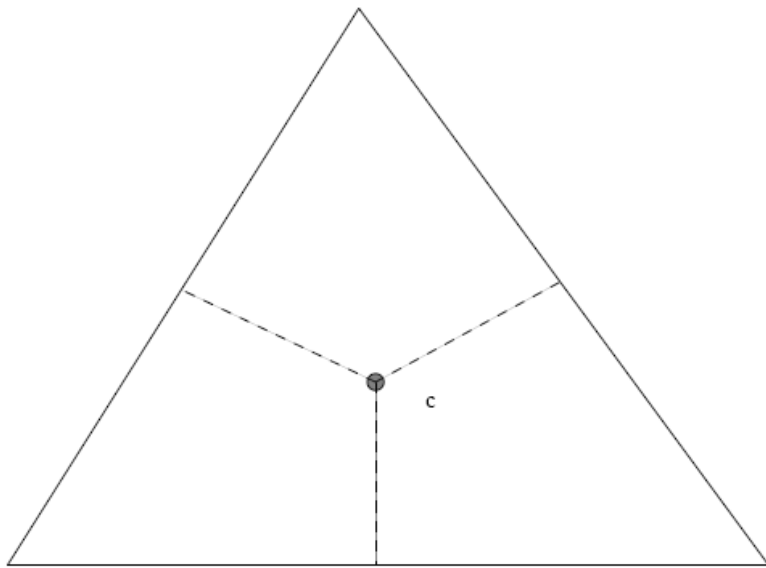
□ Mapping from physical hexahedral grid elements to a standard computational element



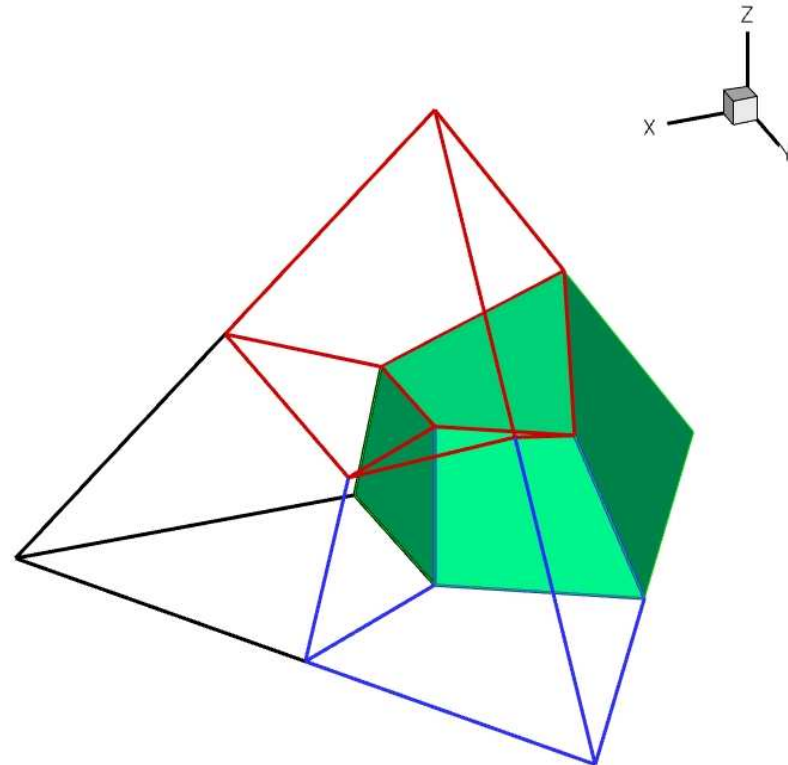
$$(0 \leq \xi \leq 1, 0 \leq \eta \leq 1 \text{ and } 0 \leq \beta \leq 1)$$



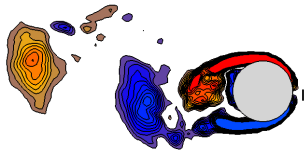
Splitting triangulated grids to quadrilateral grids in 2D and 3D



(a) A triangle split into three quadrilaterals

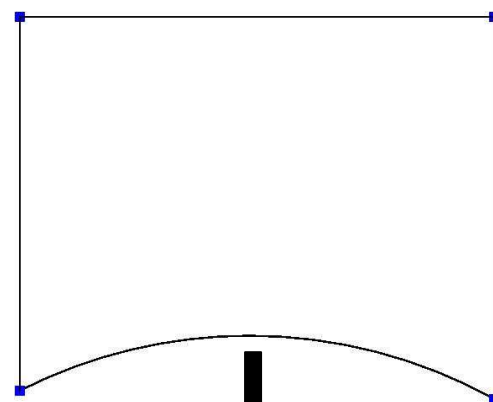


(b) A tetrahedron split into four hexahedra

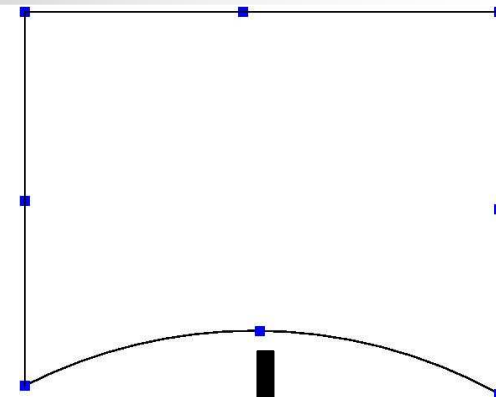
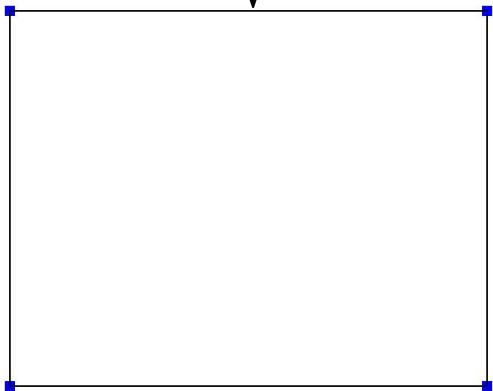


Curved wall representation

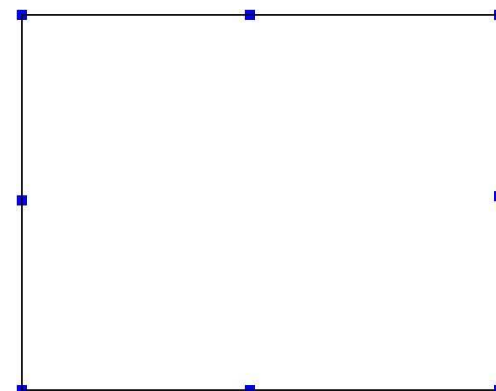
$$\begin{pmatrix} x \\ y \end{pmatrix} = \sum_{i=1}^K M_i(\xi, \eta) \begin{pmatrix} x_i \\ y_i \end{pmatrix}$$



linear



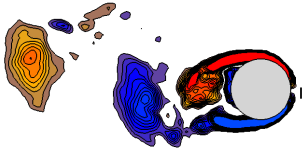
quadratic



M is shape function; K = 8, 20 for 3D linear, quadratic mapping

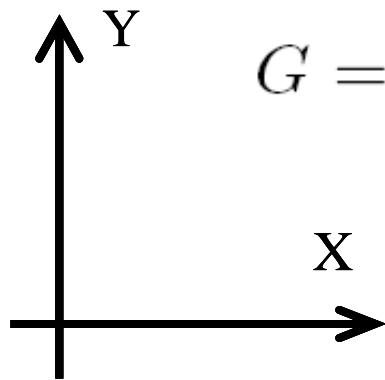
K = 4, 8 for 2D linear, quadratic mapping

Extension to Moving and Deformable Grids (I)



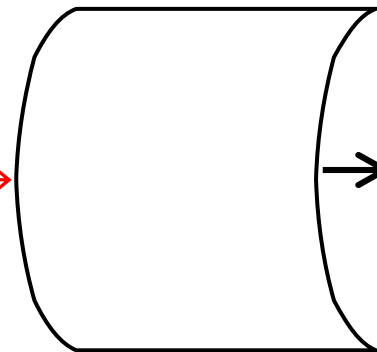
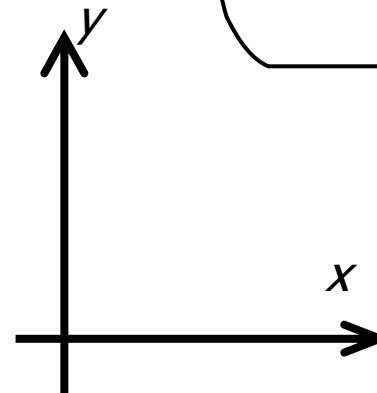
$$(x, y, z) = M(X, Y, Z, t)$$

$$G = \nabla_X M = \frac{\partial(x, y, z)}{\partial(X, Y, Z)}$$



→ NdA

G, g, w

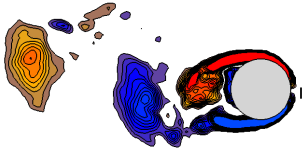


→ nda

Moving
physical
framework

Reference framework

Extension to Moving and Deformable Grids (II)

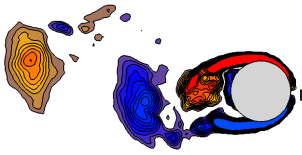


Define a mapping velocity $\frac{\partial M(X, Y, Z, t)}{\partial t} = w$
:

$$\frac{\partial \hat{Q}}{\partial t}|_X + \nabla_X \hat{F}_e(\hat{Q}) - \nabla \hat{F}_v(\hat{Q}, \nabla \hat{Q}) = 0$$

$$g = \det(\mathbf{G}) \quad \hat{Q} = gQ$$

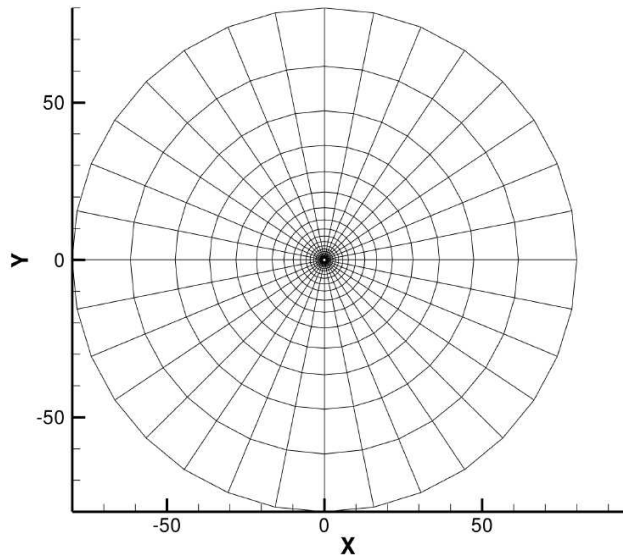
$$\hat{F} = gG^{-1}F - \hat{Q}G^{-1}w$$



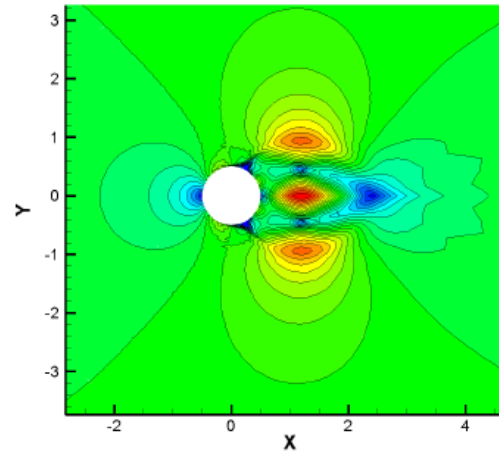
VALIDATION



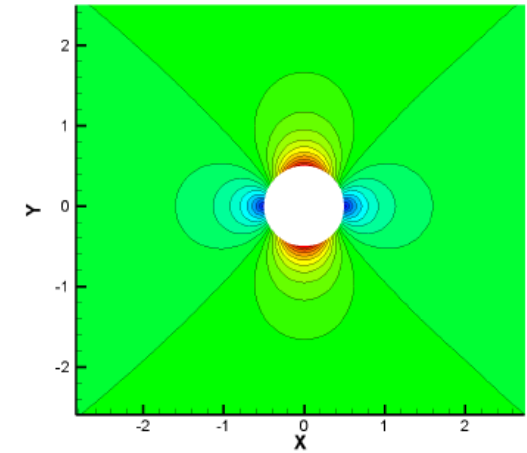
Mach contour around a circle



4th-order SD method on a grid
with 32x32 cells



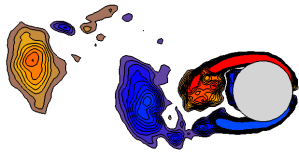
(a) linear wall boundary



(b) cubic wall boundary

□ Free stream Mach = 0.2

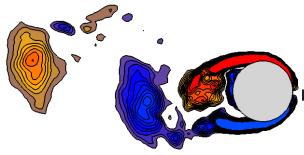
□ Inviscid Euler solver



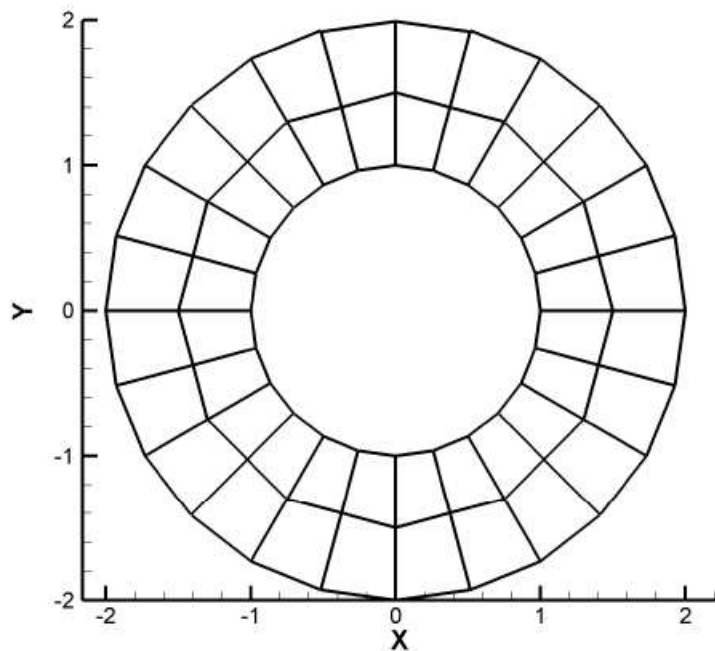
Effect of interface flux on C_d

Riemann	order	cell no.	Wall	Mach	$\Delta_t u_\infty / D$	C_d
CUSP	4th	640	quadratic	0.2	2e-4	-1.86e-5
AUSM	4th	640	quadratic	0.2	2e-4	-4.39e-5
Roe	4th	640	quadratic	0.2	2e-4	-1.03e-5
flux vector split	4th	640	quadratic	0.2	2e-4	-1.18e-5
Scalar diffusion	4th	640	quadratic	0.2	2e-4	-8.8e-6

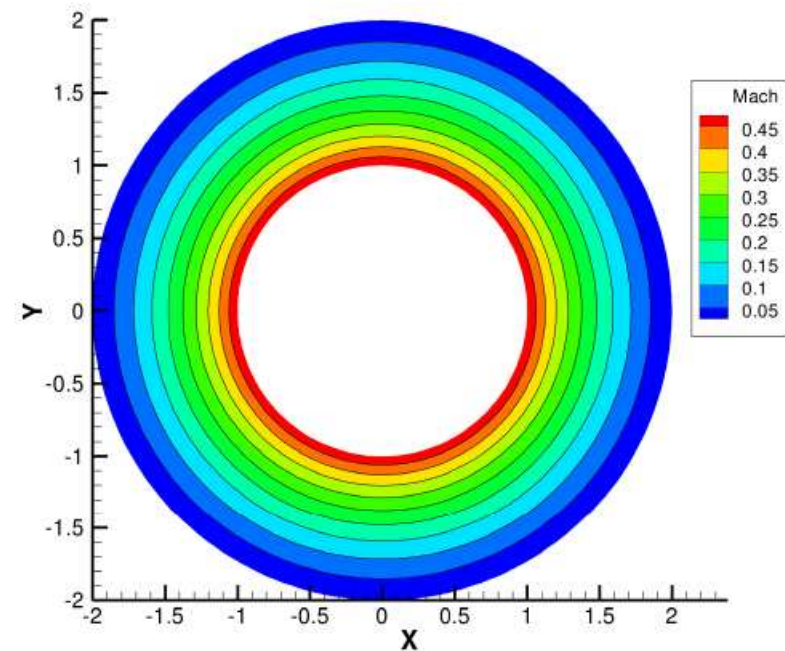
□ Inviscid flow past a circle



Compressible Taylor-Couette Flow



(a) Grid



(b) Mach contour

Mach = 0.5, $Re=10$, isothermal for inner cylinder
and adiabatic wall for outer cylinder

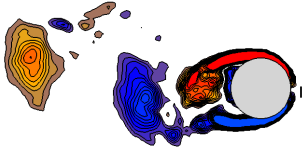


Verification of order of accuracy

No. of elements	No. of DOFs	L2-error	Order
3rd order SD			
48	432	8.896E-04	-
192	1728	1.002E-04	3.15
768	6912	1.084E-05	3.21
4th order SD			
48	768	1.4815E-04	-
192	3072	1.0036E-05	3.88
768	12288	6.5746E-07	3.93

Exact solution for
angular velocity

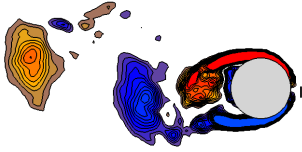
$$v_{\theta} = \Omega_i r_i \frac{\frac{r_o}{r} - \frac{r}{r_o}}{\frac{r_o}{r_i} - \frac{r_i}{r_o}}$$



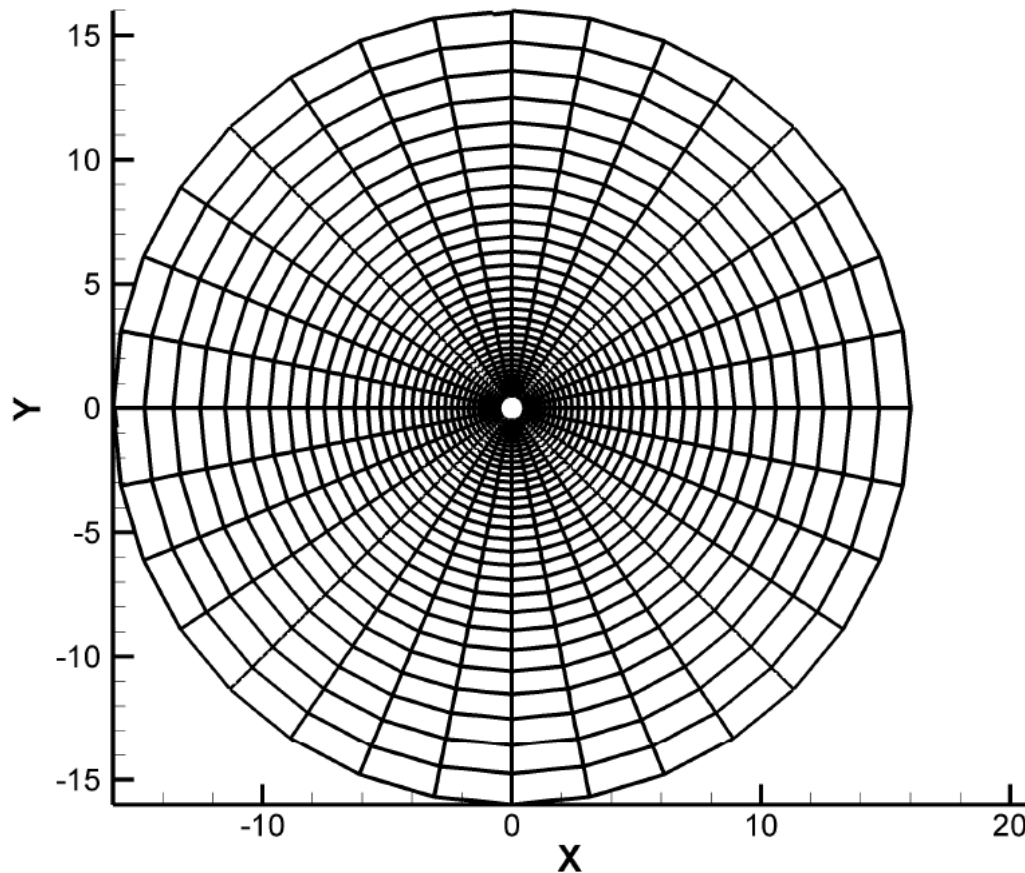
Studies of Vortex Shedding Past a Plunging Cylinder



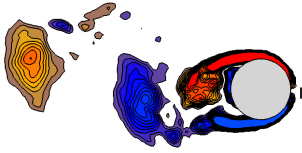
E. GUILMINEAU and P. QUEUTEY,
*A NUMERICAL SIMULATION OF VORTEX SHEDDING
FROM AN OSCILLATING CIRCULAR CYLINDER*
Journal of Fluids and Structures
Vol 16, 2002, pp. 773-794



Computational grid for oscillating cylinder



- Our simulation uses only 32x32 grid
- The third-order SD method
- Total degrees-of-freedom = 96x96
- Quadratic curved wall



vorticity shedding behind an oscillating cylinder

- $Y(t) = A_e \cos(2\pi f_e t)$
for cylinder transverse motion

- $A_e = 0.2D$

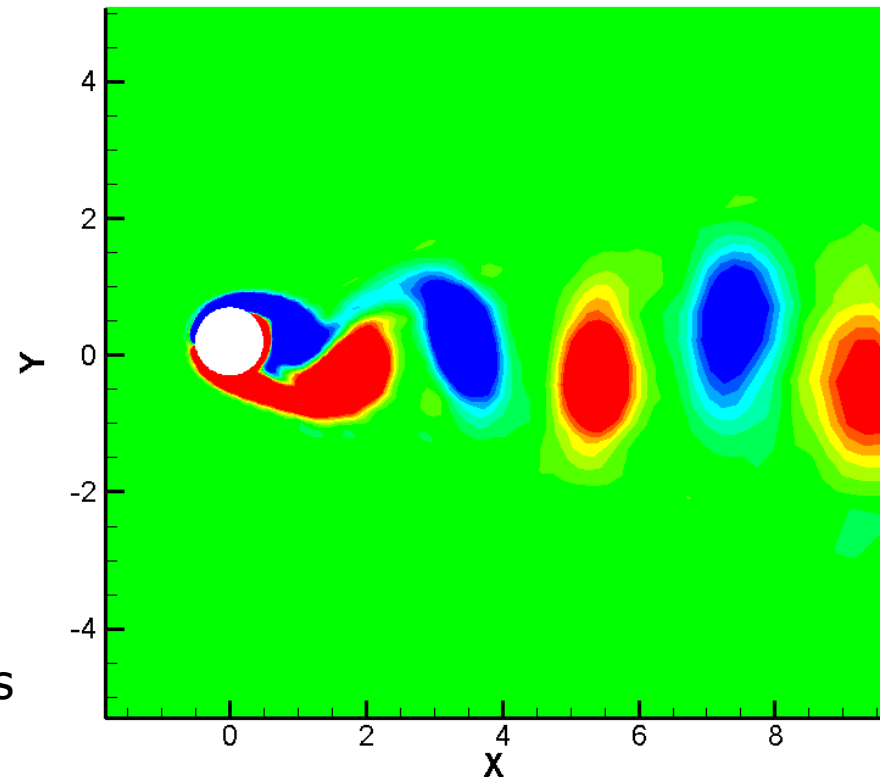
- $f_e = 1.1 f_n$

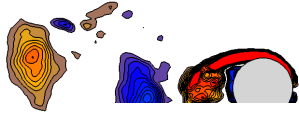
- $-1 < \omega d/U < 1$

- $Re = 185$

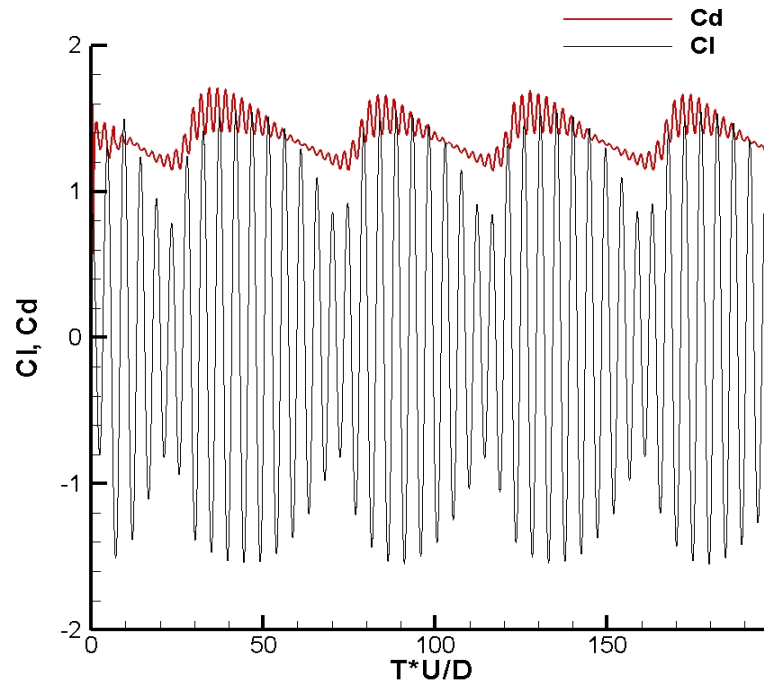
- The cylinder motion is identical to the one reported in E. GUILMINEAU and P. QUEUTEY, Journal of Fluids and Structures Vol 16, 2002, pp. 773-794

- We obtained nearly identical results using a grid with only 1024 cells compared to their 48,000 cells



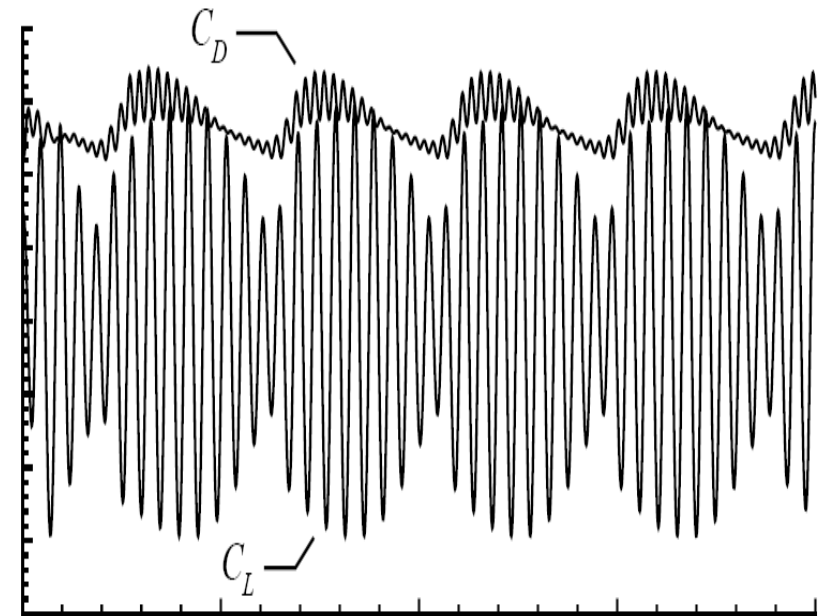


Fluid-exerted forces



(a) Third order spectral difference

Total cell : 32x32



200

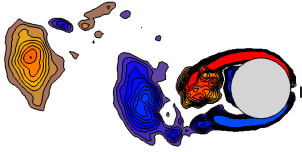
(b) E. GUILMINEAU and P. QUEUTEY

Journal of Fluids and Structures

Vol 16, 2002, pp. 773-794

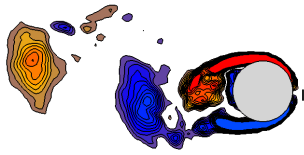
Total cell : 240x200

The predicted force coefficients are in a good agreement with Guilmineau and Queutey (2002) and much less computational cells are used.

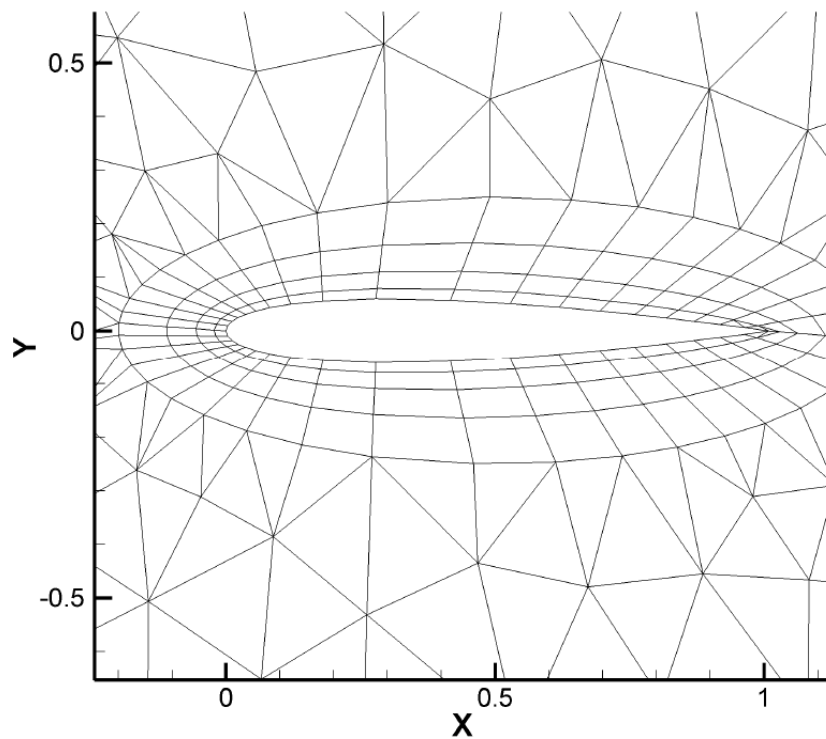


Studies of plunging airfoils

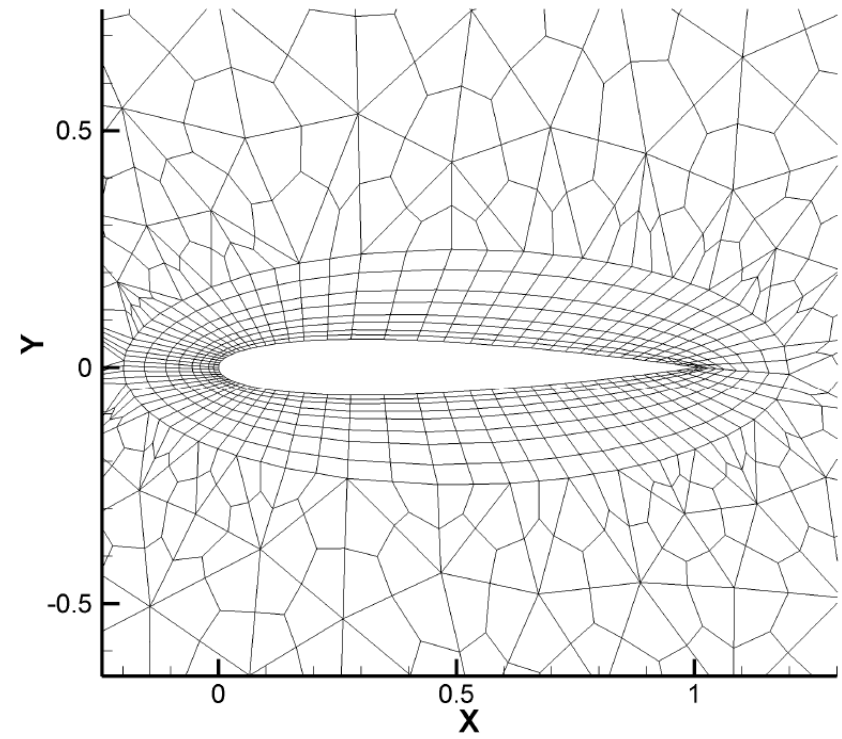
□ K. D. Jones, C. M. Dohring and M. F. Platzer,
Experimental and computational investigation of the
Knoller-Betz effect,
AIAA Journal, Vol 36, pp. 780-783.



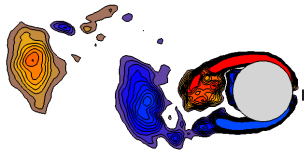
NACA 0012 grid with mixed elements



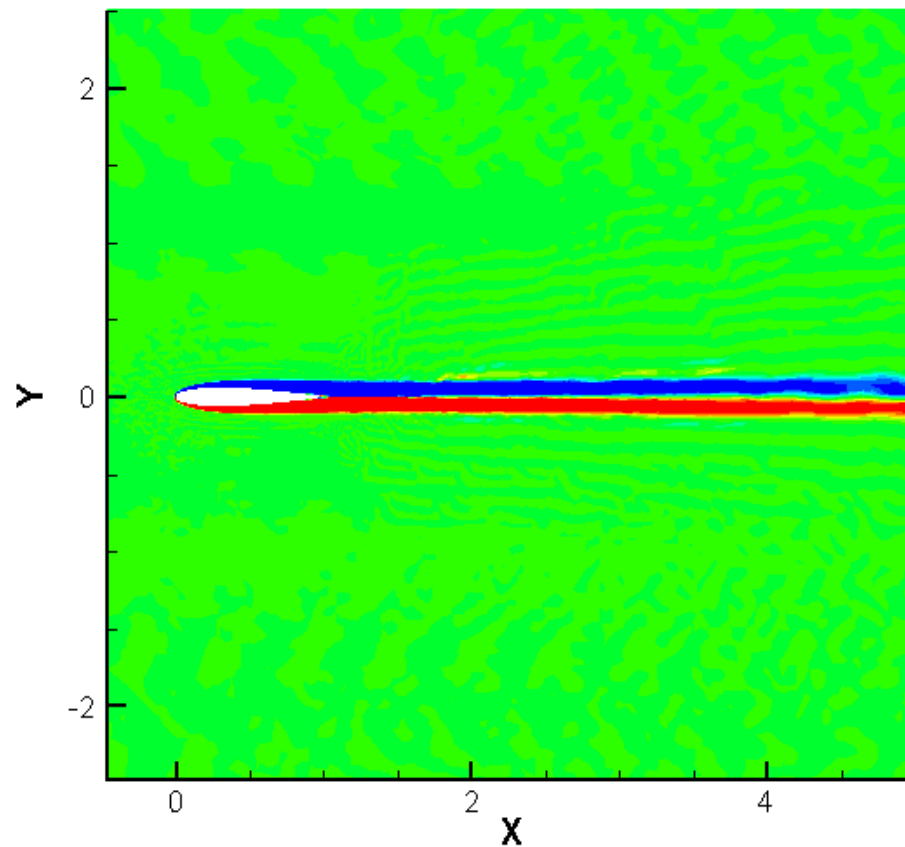
(a) Initial hybrid mesh: 'Mesh A'



(b) One-level h-refinement: 'Mesh B'



Viscous flow past a stationary airfoil



- $Re = 1850$
- $Mach = 0.2$
- Vortices:

$$-6 \leq \omega c / U_{\infty} \leq 6$$

Steady flow solution
is reached eventually



Slow plunging airfoil case

- $Y(t) = A_e \sin(\omega t)$

- $\Omega = 1.15$

- $A_e = 0.08 c$

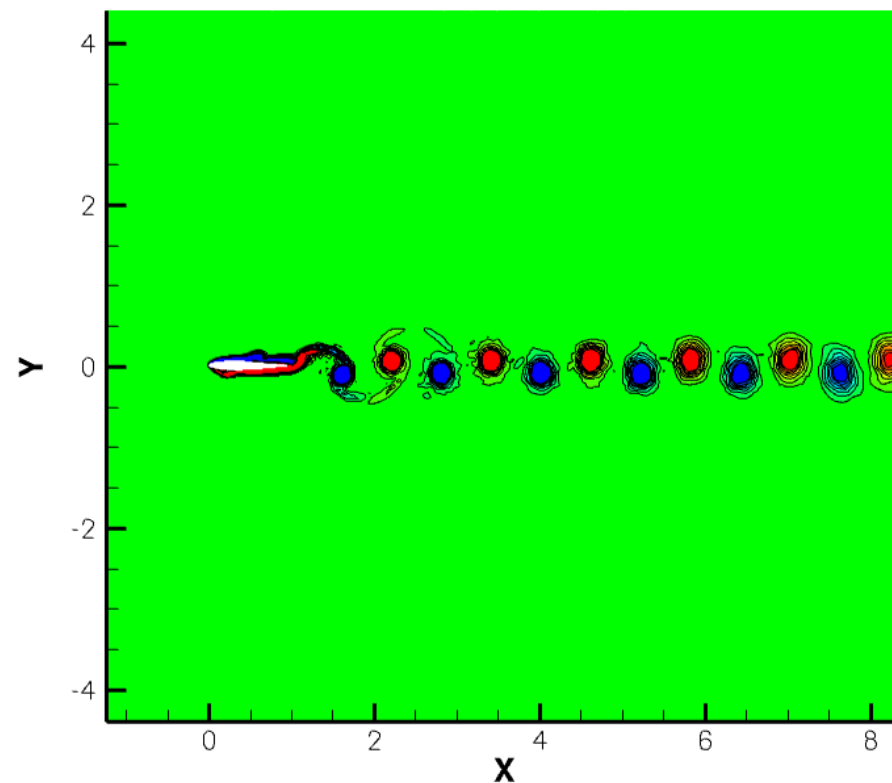
- Chord $c = 1$

- $Mach = 0.2$

- $U_{\infty} = 0.2$

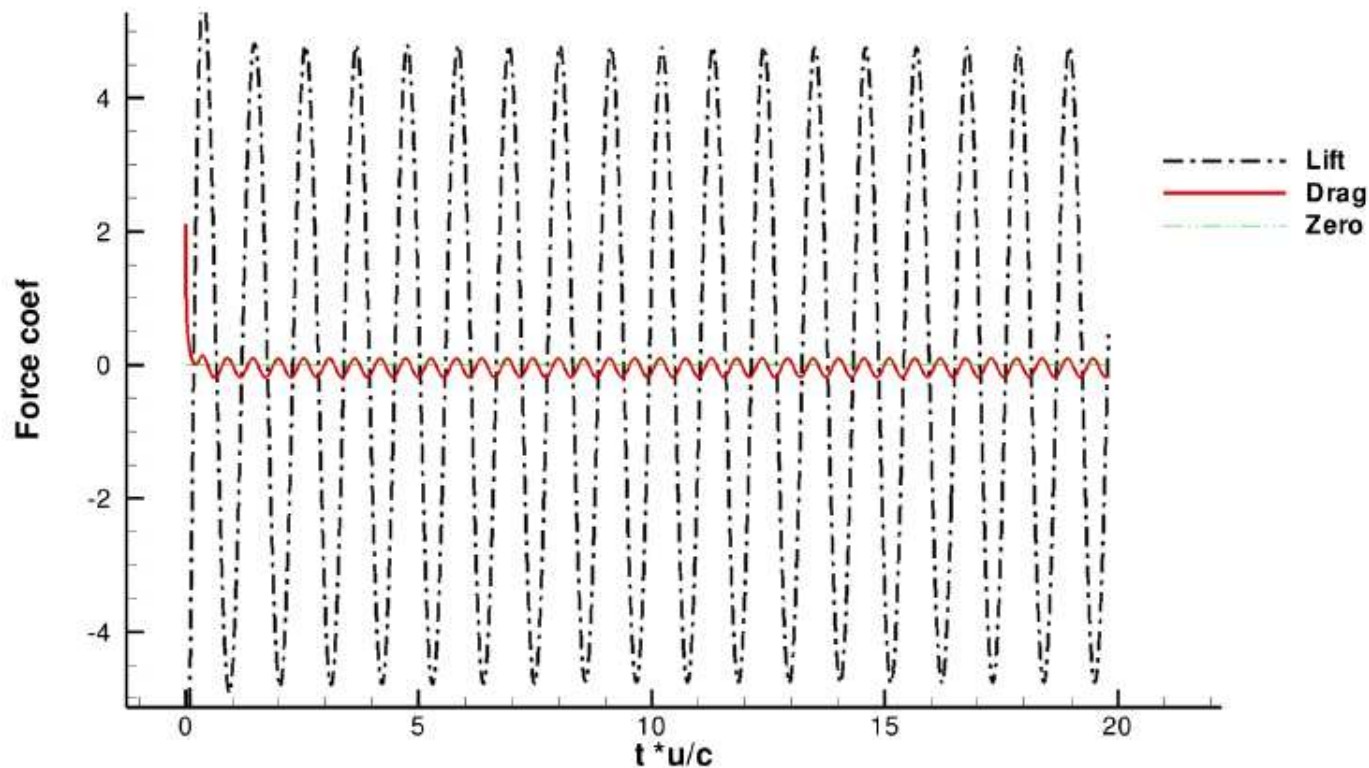
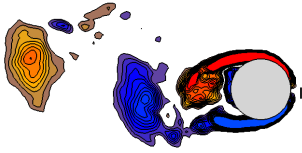
- $Re = 1850$

- 4th order spectral difference method



$$-6 \leq \omega c / U_{\infty} \leq 6$$

Force coefficients for the slowly plunging airfoil



$$-4.78 < C_l < 4.77$$

$$-0.181 < C_d < 0.1$$

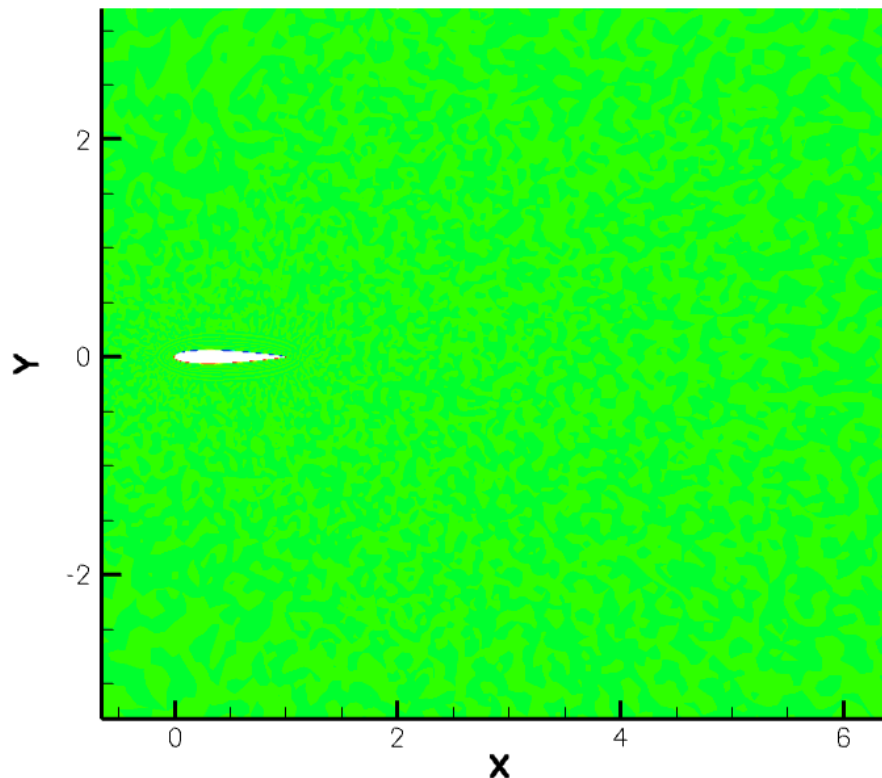
$$\text{Mean drag coef} = -0.0436$$



Fast plunging case

Our simulations suggest that the asymmetrical flow pattern depends on the direction of the airfoil's first stroke.

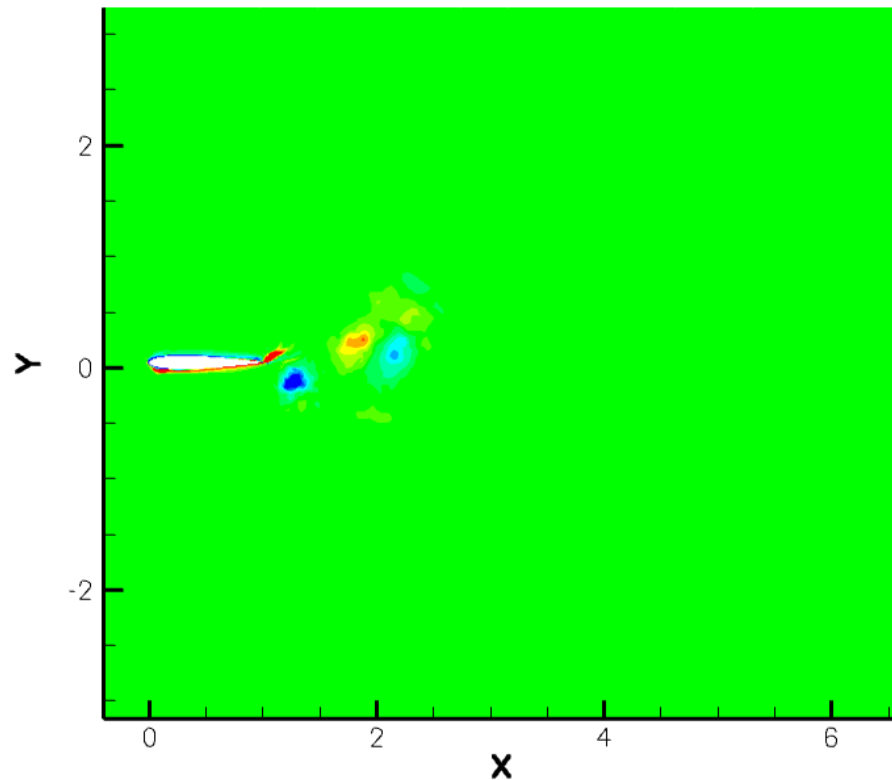
- First stroke of the airfoil goes upwards
- $Y(t) = A_e \sin(\omega t)$
- $\Omega = 2.46$
- $A_e = 0.12 c$
- Chord $c = 1$
- $Mach = 0.2$
- $U_{inf} = 0.2$
- $Re = 1850$
- 3rd order spectral difference method





Fast plunging, 3rd-order simulation

- First stroke of the airfoil goes downwards
- $Y(t) = Ae \sin(\omega t)$
- $\Omega = 2.46$
- $Ae = 0.12 c$
- Chord $c = 1$
- $Mach = 0.2$
- $U_{\infty} = 0.2$
- $Re = 1850$
- 3rd -order spectral difference method

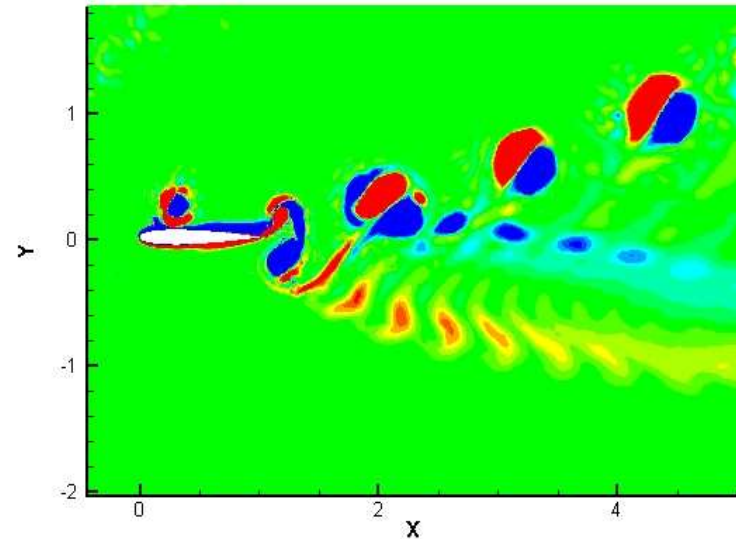




Simulation versus Experiment



(a) Experiment by Jones, Dohring, and Platzer; AIAA JOURNAL Vol. 36, No. 7, July 1998

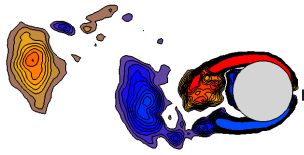


(b) 4th order Spectral difference method

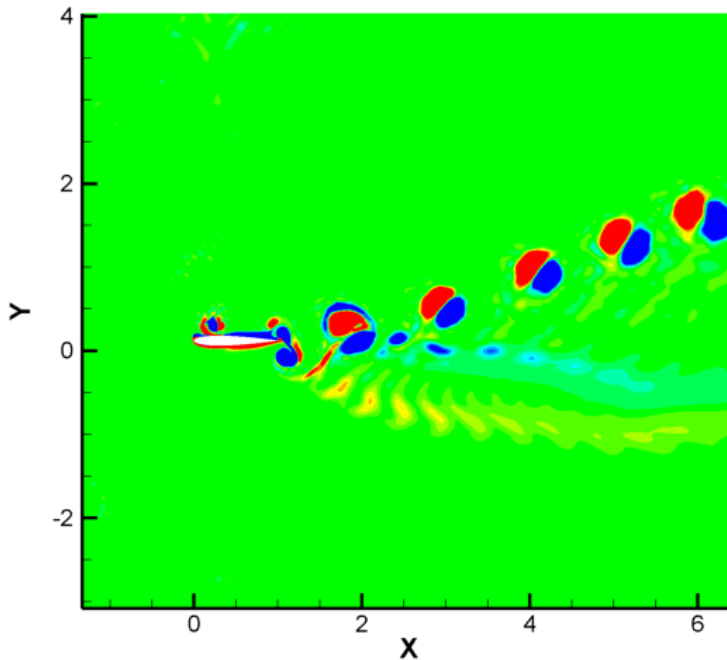
Our prediction agrees better with the experimental results than any other published results !

- First stroke of the airfoil goes downwards
- $Y(t) = Ae \cdot \sin(\omega \cdot t)$
- $\Omega = 2.46$
- $Ae = 0.12 c$

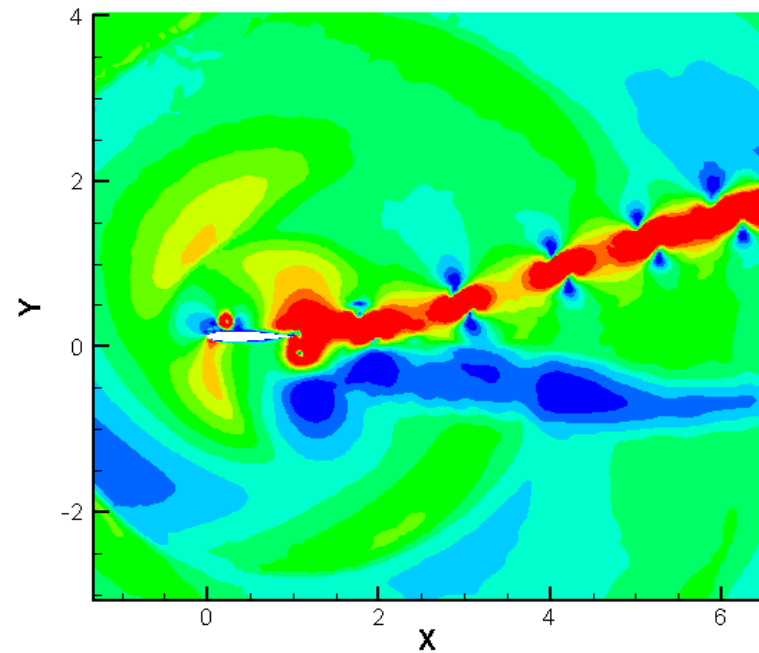
- $Mach = 0.2$
- $U_{inf} = 0.2$
- $Re = 1850$
- Chord $c = 1$



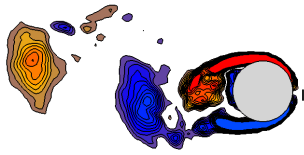
4th-order SD prediction for plunging airfoil



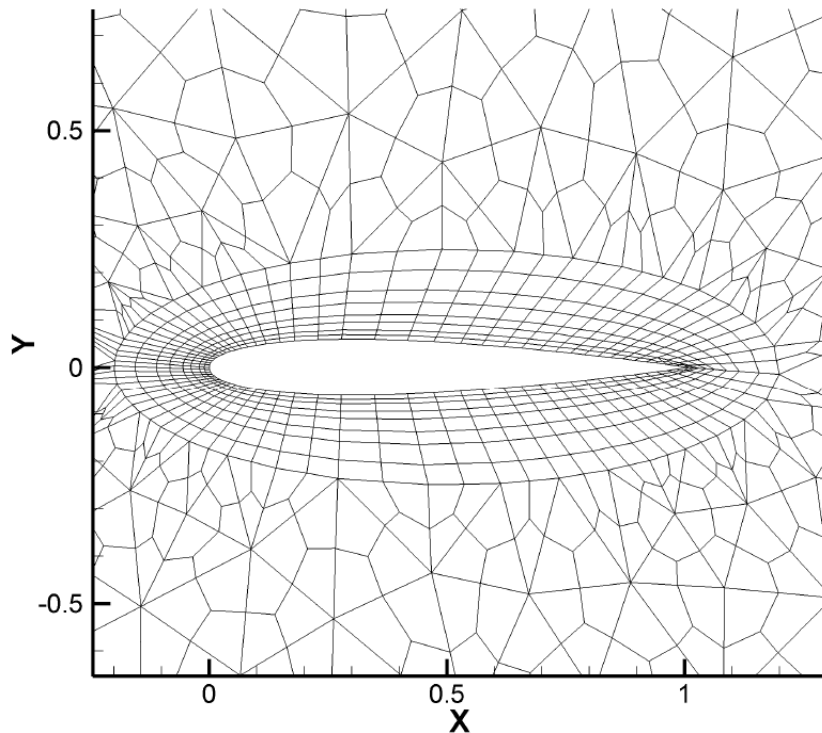
- Vorticity: $-6 < \Omega c/U < 6$
- $Y(t) = A e \sin(\omega t)$
- $\Omega = 2.46$
- $A e = 0.12 c$



- Normalized velocity magnitude:
 $0.5 < |V|/U_{\infty} < 2$



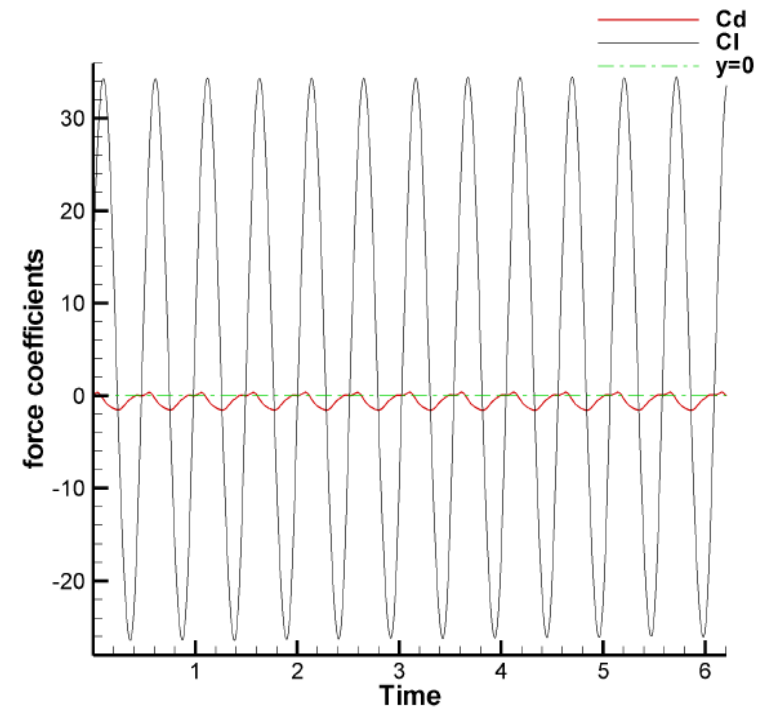
Force coefficients for fast plunging case



(a) Mesh B

$$-26 < Cl < 34$$

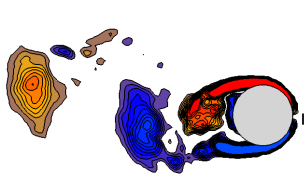
$$-1.51 < Cd < 0.37$$



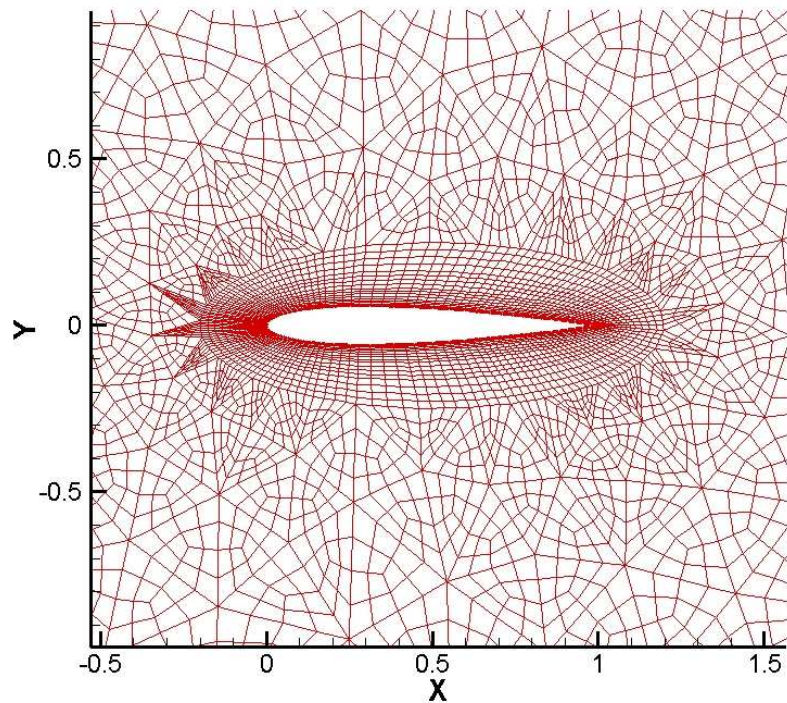
(b) the 4th order SD method;

Mean drag = -0.51

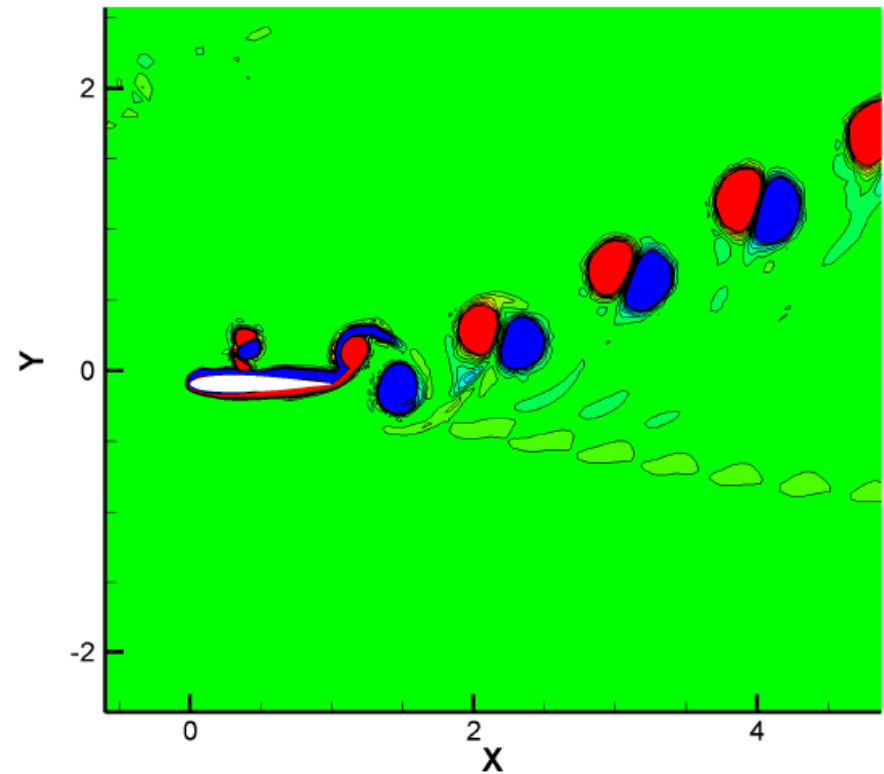
Mean lift = 2.57



Vorticity shedding on the finest mesh

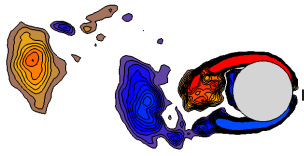


(a) Mesh C



(b) Vorticity $-6 \leq \omega c/U_\infty \leq 6$

Third-order SD method is used



Conclusions

- The SD method is robust and able to model compressible viscous flow with moving boundaries with high accuracy.
- It enables accurate simulations of vortex dominated flows
- Potential applications include flapping wing flight and wind turbine aerodynamics